(3) Ferroelectric Bolometer for Space Research

(5) Hector C. Ingrao*, Donald H. Menzel* and Frederic J. Kahn*

In this paper we offer comparisons between the ferroelectric bolometer and other thermal detectors from the point of view of space instrumentation.

We manufactured ceramic ferroelectric bolometers which have Curie points between -10°C and +10°C and dimensions down to .5mm × .5mm × 50 microns. We measured the performance of a radiation pyrometer which has a ferroelectric bolometer 1.0mm × 1.0mm × 0.2mm. With an incident infrared signal chopped at 2.5 cps, and 2 bandpass $\Delta f = 0.25$ cps, and at room temperature, the minimum detectable power W_m is 4×10^{-10} watts rms. Theoretical values of the responsivity and W_m of the detector are compared with experimental data.

There exist many observational problems in space research for which solutions can be found in the 7μ - 40μ region of the electromagnetic spectrum. Temperature measurements of planetary surfaces and atmospheres, infrared planetary albedo, etc. are among the aspects of scientific interest that we can explore in the 7μ - 40μ band.

Of special interest will be the 8μ - 14μ region since this region is a broad atmospheric window and permits observation from ground base-stations or from space vehicles, with the same type of instrument. This is particularly advantageous, for example, for measuring lunar temperatures in the same area simultaneously from a space craft close to the Moon and from similar equipment on the ground.

In experiments where it is possible to use single detectors, these detectors will fall into two main categories: quantum or thermal type.(1) For quantum detectors to operate at wave lengths in the region of our interest (8μ - 14μ), they must be used in connection with cryogenic devices. A possible exception in this category might be a detector using a mechanism discovered by Diemer.(2)** At present, however, working

Work sponsored by the National Aeronautics and Space Administration.

* Present address: Division of Engineering and Applied Physics, Harvard University, Cambridge, Massachusetts, U.S.A.

** In contrast to all other quantum infrared detectors the principle of operation of the proposed detector does not involve free carrier generation by the infrared radiation. Instead the detector uses the absorption of infrared energy by excitons to quench an exciton - induced photoconductivity.

detector based on this principle is not available.[3]

Analysis of the performance of thermal detectors shows that for space instrumentation the best detector which is commercially available is the thermistor bolometer. This detector satisfies the requirement of relatively low NEP, can be obtained in different shapes and sizes, tolerates vibration encountered during the launching of a space craft, has a time constant of milliseconds, and has a reasonable electrical impedance. Thermistor bolometers have been used successfully in the two horizon sensors in the nose of the Mercury capsule, in the 5-channel radiometer on board the Tiros meteorological satellites and in the two-channel infrared radiometer in the Mariner II spacecraft.

As one might expect, this detector has certain drawbacks too. Since the resistance of the bolometer operating at room temperature is of the order of 10^6 ohms and the corresponding bias about 50 volts, the power dissipated in the detector is about 2.5×10^{-3} watts. Since the detector has a negative coefficient, increase in the ambient temperature will reduce the resistance. Hence there is a risk of reaching a runaway point resulting in self destruction of the detector.

The irreducible noise in the thermistor is Johnson and current noise, and is well above the signal generated by the thermal statistical fluctuations of the detector itself.

A ferroelectric bolometer, operating in the pyroelectric or the dielectric mode, is under certain conditions limited only by temperature fluctuations. Cooper[4] and Hanel[5] have computed this for a detector nade of $BaTiO_3$ single crystal. Furthermore, it can operate satisfactorily over a wide range in temperature with bias from a constant voltage source. The problem of damage to the detector over a wide range in temperature (of the order of several hundred degrees centigrade) does not exist. Since the internal dc resistance is about 10^{12} ohms, the power dissipated by the bias in the detector will be about 10^{-8} watts. This a factor of 10^6 less than in the thermistor bolometer. The other important characteristic, is that the signal output under certain conditions is proportional to the derivative of the temperature of the detector with respect to time. Moreover, if the detector operates in the pyroelectric mode, it requires no external power supply for biasing.

Planetary problems lead us to investigate various schemes for image forming systems. In the course of this work and as part of the effort to develop a thermal image-forming system of simultaneous read-in for lunar observations,[6] our laboratory has built and tested several single thermal detectors using the combined pyroelectric and dielectric variations of $(Ba, Sr)TiO_3$ solid solutions as a function of the temperature near the Curie point.[1][7] Our current detectors are made of a $Ba(Ti, Sn)O_3$ with the addition of various impurities including rare earths.

When we began our program in 1960, we did not know that other laboratories were working in this field. We have since learned that Burns[8] has analyzed the possibility of a thermal image tube using ferroelectric material as a target plate. Mattes and Perals[9] have made a pyroelectric transducer of $BaTiO_3$ ceramic for measuring large temperature changes of tens of degrees. Lang[10] reported that by using pyroelectric phenomena in a rod of $BaTiO_3$ ceramic, temperature changes of 2×10^{-7} °C could be detected. More recently the Boeing Co.[11] analyzed, theoretically and experimentally, ferroelectric bolometers in the pyroelectric and dielectric modes of operation. They used two different crystals, potassium dihydrogen

phosphate (KDP) and triglycine sulphate (TGS). The KDP has a Curie point at 123°K and the TGS, at 498°C. The best result that Boeing obtained was with the TGS detector operating at 248°K. They obtained an NEP of 8.1×10^{-9} watts per 5cps. bandwidth.

A thorough theoretical analysis of the performance of the device will be published elsewhere.* In this paper we will briefly summarize the results of this analysis.

We first consider the heat balance of the ferroelectric bolometer. The equivalent circuit of the detector operating at a temperature T_o is given in figure 1. The detector element is represented by capacitor C_D in parallel with an equivalent leakage resistor R_D. E_{bb} is an external battery bias for the detector and R_L is the real part of the input impedance of the electrometer used to measure the current output of the detector. The detector output (i) is measured as fluctuations in I_L. W is the infrared signal input to the detector.

We can describe the thermal behavior of the detector by a first order linear differential equation in time with constant coefficients and a time varying forcing function which is, to the first order, the energy input to the system. The thermal response of the system for a given input may be found from:

$$\theta = \mathcal{L}^{-1}\left[\frac{\mathcal{R}\,\underline{W}}{(1+p\tau_t)}\right] \qquad (1)$$

where θ is the deviation of the average detector temperature from the steady state value, $\underline{W}$ is the Laplace transform of the radiation input to the detector, $\mathcal{R}$ is the equivalent thermal resistance, τ_t is the thermal time constant, p is the differential operator, and $\mathcal{L}^{-1}$ is the inverse Laplace transformation operator. For typical detector parameters this expression will be accurate to less than one percent for all radiation inputs below 5000 watts cm^{-2},

The electrical response of the detector is described by the network node equation - a first order linear differential equation in time with variable coefficients and a time varying forcing function determined by the radiation input. In the linear region of the dielectric or for small θ in a non-linear region we may write

$$C_D = C_o + a_1\,\theta \qquad (2)$$

$$P_s = P_o + a_2\,\theta \qquad (3)$$

where C_o is the detector capacitance and P_s is the spontaneous polarization of the dielectric. Inserting equations (1), (2), and (3) in the node equation, we can obtain the detector output for any given radiation input.

The most direct solution is by harmonic analysis. Here we assume an input of the form

---

* Scientific Report on NASA Grant 64-60 in press by Harvard College Observatory.

$$W = W_o \; e^{j\omega t} \tag{4}$$

and solve for an output of the form

$$v = \sum_{n=1}^{\infty} V_n \; e^{jn\omega t} \tag{5}$$

where v is the time varying component of V_L. The first order transfer function V_1 of the network may be used, through Laplace techniques, to generate solutions for the outputs due to non-sinusoidal inputs. Two special cases of particular interest are the responses to the step input

$$W = W_o \; U(t) \tag{6}$$

and the ramp input

$$W = kt \tag{7}$$

In this manner we find for the sinusoidal input, given by equation (4), the following solution:

$$v = \frac{\omega \lambda W_o \; e^{j[\omega t - \pi/2]}}{(1 + j\omega\tau_t)(1 + j\omega\tau_e)} \; . \tag{8}$$

where $\lambda = IR\, R_E \left[\alpha_1 \left(R_D z / R_D + R_L \right) E_{bb} + \alpha_2 A \right]$, (9)

$\frac{1}{R_E} = \frac{1}{R_D} + \frac{1}{R_L}$, A = the area of each detector electrode and

τ_e = the electrical time constant of the network.

The n th order harmonic is given by

$$v_n = n! \left(\frac{-j\omega\alpha_1 IR\, R_E W_o}{1 + j\omega\tau_t} \right)^n \frac{\lambda e^{jn\omega t}}{(\alpha_1 IR\, R_E)(1 + jn\omega\tau_e)[1 + j(n-1)\omega\tau_e] \cdots (1 + j\omega\tau_e)} \tag{10}$$

For radiation inputs below 3×10^{-2} watts cm^{-2}, consideration of only the first harmonic yields accuracy within one per cent.

For the step input of equation (6),

$$v = \frac{\lambda W_o}{\tau_t - \tau_e} \left(e^{-t/\tau_e} - e^{-t/\tau_t} \right) \; . \tag{11}$$

where we note that when $\tau_t >> \tau_e$ the rise time will be approximately τ_e and the fall time approximately τ_t. For power inputs above 3×10^{-4} watts cm^{-2} we may expect non-linear effects in the detector to become significant, probably in the form of higher order transients, e.g. e^{-2t/τ_e}, e^{-3t/τ_e}. Hence for high signal levels, we may expect significantly shorter rise times than τ_e.

We may define the voltage responsivity for step function by

$$r_{v,\,step} = \frac{v_{max}}{W_o} \tag{12a}$$

and the current responsivity by

$$r_{I,\,step} = \frac{i_{max}}{W_o} \quad . \tag{12b}$$

Typically we may have $\tau_e << \tau_t$.
Then if $R_E \simeq R_L$, we find from equations (9), (11) and (12b)

$$r_{I,\,step} \simeq \frac{a_1 E_{bb} + a_2 A}{C} \tag{13}$$

where C is the equivalent heat capacitance of the detector. It is important to note in equation (13) that the current responsivity is dependent only on the applied bias and the characteristics of the device itself, and not on the electrical parameters of the associated electronics. This is of course provided $\tau_e << \tau_t$. Equation (13) would seem to indicate that for $T < T_c$ the detector responsivity $r_{I,\,step}$ is directly proportional to the bias voltage E_{bb} . This will be true, however, only for the linear region of the detector where $a_1 \simeq$ constant and where $\omega << 1/\tau_e$ (for a sinusoidal input).

In general, the dielectric constant and hence both C_o and a_1 will be functions of the stresses introduced by the electric field originated by E_{bb} . An increase in electric field will decrease the dielectric constant.

The optimum value of E_{bb} to be used is decided on the basis of maximizing the responsivity. Other analyses have indicated dielectric breakdown due to E_{bb} to be the limiting factor. However, it is the field dependence of a_1 and C_o that will determine the point of operation. The electric fields used in our detectors range from 0.5×10^6 to 1.6×10^6 volts per meter.

From measurements on barium-strontium titanate ceramic (25% $SrTiO_3$, 75% $BaTiO_3$)* we see that at these field strengths, K' has decreased to 65% and 30% of its zero value respectively. The thermal point of operation of the detector depends on the characteristics of the ferroelectric material itself. In the case of material used in our bolometers and for operation above the Curie point, the responsivity will be practically constant throughout the range of 10°C to 25°C. The general response to the ramp input expressed by equation (7) will be

$$v = -\frac{\lambda K}{\tau_t - \tau_e}\left[\tau_e\left(e^{-t/\tau_e} - 1\right) - \tau_t\left(e^{-t/\tau_t} - 1\right)\right] \tag{14}$$

an expression which is best interpreted by considering three special cases.

---

* S. Roberts, "Dielectric and Piezoelectric Properties of Barium Titanate". Phys. Rev. 71 892, 1947.

For $t \ll \tau_t$ and $t \ll \tau_e$

$$v = 0 \tag{15}$$

to the 1st order in time.

$$v = \lambda K \left(\frac{t}{\tau_t - \tau_e}\right)^2 \tag{16}$$

to the 2nd order in time.
When $t \ll \tau_t$ and $t \gg \tau_e$ equation (14) becomes:

$$v \simeq -\frac{\lambda K}{\tau_t - \tau_e}(t - \tau_e) \simeq -\lambda K\left(\frac{t}{\tau_t}\right) \tag{17}$$

and finally for $t \gg \tau_t$, $t \gg \tau_e$

$$v = -\lambda K \simeq -\frac{\lambda}{IR}\frac{\partial \theta}{\partial t} \tag{18}$$

or alternately

$$i = -\left(a_1 E_{bb} + a_2 A\right)\frac{\partial \theta}{\partial t} \tag{19}$$

Thus we see in equation (15), the detector output for a ramp input will be null to the first order in time for all times shorter than τ_e and τ_t , as the result of the combined effects of electrical and thermal damping.

For times much greater than τ_e , equation (17), the output is directly proportional to time and to the slope of the input ramp. Finally for times greater than τ_e , equation (18), we find the detector output will be constant for a given ramp input. This output will be proportional to the slope of the ramp and thus in turn to the change in detector temperature with respect to time. Equation (19) displays explicitly the independence of the output current from the electrical parameters of the associated electronics and is analogous to equation (13) which gives the current responsivity for a step function.

We will describe some of the experimental results for a ferroelectric bolometer operating in the dielectric mode. This bolometer was made of $Ba(Ti, Sn)O_3$ solid solution with a Curie point at approximately +5°C. The bolometer is identified with the Serial No. G-20311 and Table I provides the relevant physical data. Figure 2 gives the capacitance C_D and loss tangents as a function of temperature for the same bolometer. Figure 3 shows a detector flake and figure 4 shows a complete bolometer. We tested the bolometer at the infrared bench where a square wave signal at a continuously variable frequency or a step function can be generated. Figure 5 gives the block diagram of the electronic setup for testing the ferroelectric bolometer in dc and ac operation. The rise time of the electrometer for the actual working conditions is 70 milliseconds. The General Radio Vibration Analyzer provides a very narrow band pass that is a percentage of the tuning frequency. Figure 6 shows the response of detector No. G-20311 to a negative and positive infrared step function. The bias is 330 volts, the room temperature 28.5°C* and the step signal 7.5×10^{-6} watts. The chart speed is 1mm per second; noise level is determined by

* The room temperature was undesirably high due to a malfunctioning of the airconditioning system.

the electronics. Figure 7 shows the output of bolometer No. G-20311 in ac operation. The signal input is a 5.8×10^{-9} watts peak-to-peak square wave. Chopping frequency is 2.5cps; bandwidth, 0.25cps; chart scale; approximately 3.2×10^{-10} watts per division. The noise level is seen as slow fluctuations in output amplitude.

At 32°C room temperature and with a bias of 120 volts on the same detector, we obtained a new series of oscillograms in ac modes of operation. Figure 8 shows response for chopping frequencies of 0.78 cps, 1.56cps, 3.3cps and 6.2cps respectively.

To evaluate the responsivity of the detector we introduce parameters corresponding to the operational ferroelectric bolometer listed in Table I under Serial No. G- 20311 The detector is cooled by radiation through a black layer (emissivity = 1) on its upper surface and by conduction through the glass backing and leads. The effect of cooling by radiation can be expressed mathematically by a radiation conductance (G_r) which at room temperature will have the value

$$G_r = 5.8 \times 10^{-6} \text{ watt } ^\circ\text{C}^{-1}$$

The lead conductance will be inversely proportional to the square root of the chopping frequency and at 10cps:

$$G_l = 5.6 \times 10^{-7} \text{ watt } ^\circ\text{C}^{-1}$$

Furthermore for the bolometer G-20311 the thermal conductance due to heat transfer through the flake base to the glass backing will be of the order of

$$G_b = 1 \times 10^{-3} \text{ watt } ^\circ\text{C}^{-1}$$

assuming a linear gradient across the detector flake and the cement bonding the flake and the glass. Thus the predominant cooling in this detector is due to G_b and the total thermal resistance is

$$R = 1 \times 10^{3} \text{ watt}^{-1} \, ^\circ\text{C}$$

For the heat capacity C of the detector G-20311 we consider only the contribution of the dielectric mass, neglecting the mass of the electrodes and black layer and the equivalent heat capacity due to the glass backing. Taking the specific heat of the dielectric to be $C_p = 0.12$ cal g^{-1} $^\circ\text{C}^{-1}$ * we find $C = 5 \times 10^{-4}$ joules $^\circ\text{C}^{-1}$. With these values we obtain a thermal time constant

$$\tau_t = RC = 0.5 \text{ second.}$$

Experimentally we found $\tau_t =$ 4 seconds. Because of the many assumptions and estimates of physical quantities involved in the computation of C and R we consider these two values to be in reasonable agreement. From direct measurement we also obtained the electrical time constant for the point of operation indicated in Table I :

---

* A.G. Chynoweth, "Dynamic method for measuring the pyroelectric effect with special reference to Barium Titanate", J. App. Phys., 27, 78, 1956.

$$\tau_{e,exper.} = 70 \text{ milliseconds}$$

The equivalent load resistance R_L is determined by the real part of the equivalent input impedance of the electrometer. The electrometer employed is a Keithley No. 417*. Using the capacitance C_D of the detector, 140 $\mu\mu f$ extrapolated at 28.5°C and the measured rise time of 70 milliseconds, we estimate:

$$R_E \simeq R_L = 3.3 \times 10^8 \text{ ohm.}$$

Extrapolating from the measurements of C_D vs T (Figure 2), obtain for the detector no. G-20311 at 28.5°C

$$\alpha_1 = 1.6 \times 10^{-11} \text{ farad °C}$$

Taking the computed value $\tau_t = 0.5$ second and the measured value $\tau_t = 70$ milliseconds, we obtain the voltage responsivity r_v to an infrared step function.

$$r_{v,theor.} = 3.5 \times 10^3 \text{ volt watt}^{-1}$$

and the current responsivity

$$r_{I,theor.} = 10.6 \times 10^{-6} \text{ ampere watt}^{-1}$$

The voltage respensivity obtained experimentally under the same conditions is

$$r_{v,exper.} = 2.33 \times 10^3 \text{ volt watt}^{-1}$$

and the corresponding current responsivity

$$r_{I,exper.} = 7 \times 10^{-6} \text{ ampere watt}^{-1}$$

This is 66% of the theoretical responsivity just computed. Since the particular detector on which those measurements were made had a black layer of camphor soot which did not completely cover the detector surface, it is not unreasonable to expect that the device was working at less than 70% of theoretical efficiency. After noting the approximations which have been made in this analysis and possible instrumental sources of error such as that due to the spectral convolution between the detector window transmittance and black body emittance of the radiation source, we find that the agreement between the experimental and theoretical responsivities is extremely good.

The minimum detectable input power will be determined by the noise inherent in the ferroelectric detector element and its associated electronics. Temperature (thermal fluctuation), Johnson, shot, flicker, partition, current, and Barkhausen noise, require consideration. For a properly designed electrometer, only noise originated in the electrometer tube itself or the input resistor will be significant. It is convenient to define the minimum detectable power by

---

* Keithley Instruments, "Instruction Manual Model No. 417 Picoammeter", 1963.

$$W_m^2 = W_T^2 + r_I^{-2} v_N^2 \tag{20}$$

or equivalently

$$W_m^2 = W_T^2 + r_I^{-2} i_N^2 \tag{21}$$

where W_T = rms noise power due to thermal fluctuations (temperature noise).

r = detector responsivity.

v_N = rms noise voltage due to all electrical sources.

i_N = rms noise current due to all electrical sources.

W_m = rms minimum detectable power.

Although it will actually be possible to detect signals smaller than W_m, the minimum detectable power as defined will serve as a good figure of merit for the system.

We computed for the bolometer No. G-20311 the noise power W_T due to thermal fluctuations at a temperature $T = 302°K$ and $\Delta f = 0.25$cps giving a value of 3.6×10^{-11} watts. For the conditions of our measurements we computed the power W_J due to Johnson noise. Taking $R_e = 3.3 \times 10^9$ ohms, $R_e C = 7 \times 10^{-2}$ seconds and $r_v = 2.33 \times 10^8$ volts watt^{-1} ; for $\Delta f = 0.25$cps we obtained $W_m = 3.4 \times 10^{-10}$ watts. Taking the proper set of values from our experimental setup we computed flicker noise, shot noise of the grid current of the electrometer tube and the reduced shot noise (anode shot and partition) for the same tube. All the values are given in Table II. Additional noise sources include the dielectric analog of Barkhausen noise associated with the domain walls, current noise due to fluctuations of the resistance of the dielectric, and battery noise due to fluctuations in the bias potential. Both the Barkhausen and current noises warrant further investigation. It is noted however that the Barkhausen noise is not important above the Curie point due to the absence of domain watts.

The battery noise is below an equivalent power of 1.0×10^{-10} watts as determined by direct measurement of the circuit noise with and without the battery connected.

Assuming these last three noise sources to have negligible contributions, the theoretical minimum detectable power for the detector analyzed under the present experimental setup will be $W_m = 3.5 \times 10^{-10}$ watts. The noise level measured was 4.2×10^{-10} watts rms. and compares extremely well with the computed value. It is noted that the minimum detectable power for the detector and experimental conditions being analyzed is determined mainly by Johnson noise.
We can show for $R_D >> R_L$

$$W_J^2 = \frac{v^2 J}{r_v^2} = \frac{4KT\Delta f}{R_e} \frac{\left(1 + 1/\omega^2 \tau_t^2\right)}{\left(a_1 E_{bb} + a_2 A\right)^2} . \tag{22}$$

which reduces for $\tau_t \gg \tau_e$ and $w\tau_t \gg 1$ to

$$W_J^2 = \frac{4KT\Delta f}{r_{I.step}^2}\left(\frac{1}{R_e}\right). \qquad (23)$$

Thus, at constant temperature, W_J may be reduced by increasing R_e or by using an electrometer with slower response ($\tau_e = R_e C$ and C is determined almost entirely by the external circuit).
Thus unless it is possible to improve the responsivity we must compromise between minimization of Johnson noise and τ_e .

We conclude by showing now it might be possible to improve responsivity in future detectors.

We can express the current responsivity to a step function as:

$$r_{I.\,step} = \frac{1}{d\rho c_p}\left(\frac{E_{bb}}{d}\frac{\partial \epsilon}{\partial T} + \frac{\partial P}{\partial T}\right) \qquad (24)$$

where

c_p = specific heat (heat capacity per unit volume)

and ρ = mass density of the dielectric material.

Thus for a given material, responsivity will be increased by reducing the thickness d of the detector flake.

The authors wish to acknowledge the valuable assistance of Mr. Daniel Malaise (Astrophysical Institute, Liege, Belgium) for some of the measurements. Mr. Malaise is working in our infrared project with the assistance of the U.S. National Academy of Sciences and C.O.P.E.R.S.

References

1. H.C. Ingrao and D.H. Menzel, "Instrumentation for Observations of Planets in the Far Infrared" Memoi res Soc. R. Sc. Liege, Cinquiemeserie, TomeVII.
2. G. Diemer, G.J. van Gurp and W. Hoogenstraaten, Phillip Res Repts. 13, 458 (1958) and 14, 11 (1959).
3. W.D. Brennan, "Uncooled IR Detector for the Ten Micron Region" Report No. ARF-1208-12A, Feb. 25, 1963 - Armour Research Foundation.
4. J. Cooper, "Minimum Detectable Power of a Pyroelectric Thermal Receiver", Rev. Sci. Instr., 33, 1, 92, 1962.
5. R.A. Hanel, "Dielectric Bolometer, A New Type of Thermal Radiation Detector", J.O.S.A., 51, 2, 220, 1961.
6. Hector C. Ingrao and D. H. Menzel "Study of Infrared Instrumentation for Thermal Photography of the Moon" Semiannual Status Report No. 2, NASA Grant NsG-64-60, Harvard University, July to December 1960.
7. H.C. Ingrao and D.H. Menzel, "Infrared Work at Harvard College Observatory", Informal Infrared Astronomy Symposium, Nov. 11, 1961, Lab. of Astrophysics and Physical Meteorology, The Johns Hopkins University Baltimore, Maryland.

8. Jay Burns, "Thermal Image Tube", Chicago Midway Laboratories, The University of Chicago, June 1956.
9. B.L. Mattes and T.A. Perals, "Transducer for the Measurement of Thermal Power", Rev. Sci. Instr., 32 3, 332, 1961.
10. S. B. Lang, "Temperature, Its Measurement and Control in Science and Industry", 27-31 March 1961, Fourth Symposium on Temperature, Columbus, Ohio.
11. Boeing Co., "Study of Advanced Solid State Infrared Detection" Final Report Contract No. AF 33(616)-7549 U.S. Air Force, November 1962.

TABLE I

CHARACTERISTICS OF A FERROELECTRIC BOLOMETER
(SERIAL NO. G-20311)
DEVELOPED AT HARVARD COLLEGE OBSERVATORY

Size (mm × mm)		1.0 × 1.0
Thickness of Dielectric (mm)		0.2
Material		$Ba(Ti,Sn)O_3$
Curie Temp (°C)		+5
Electrodes		Silver
Black Layer		Camphor Soot
Backing		Glass
Lead Material		Pt
Lead Diameter (microns)		12
Lead Length (mm)		5
Capacitance ($\mu\mu f$)		140*
Thermal time Constant (sec)	Computed	0.5
	Measured	4.0
Operating Voltage (volt)		330
Operating Field (volt cm^{-1})		1.65×10^4
Pressure (mmHg)		5×10^{-5}
Window		BaF_2
Current responsivity (amp $watt^{-1}$)	Computed	10.6×10^{-6}
	** Measured	7×10^{-6}
	Computed	3.5×10^3
Voltage responsivity (Volt $watt^{-1}$)	** Measured	2.33×10^3
Electrical Time Constant (sec)	Measured	0.070
Load Resistor (ohm)	Computed+	3.3×10^6

* Extrapolated, value for 28.5°C measured at 1Kcps and 100 volt cm^{-1} field strength
** Responsivity for step input signals.
\+ Computed on the basis of the measured rise time.

TABLE II

THEORETICAL NOISE POWERS FOR A CERAMIC $Ba(Ti,Sn)C_3$ FERROELECTRIC BOLOMETER

Source	Noise* (watts rms)
Thermal	$.36 \times 10^{-10}$
Johnson	3.4×10^{-10}
Reduced Shot (anode shot and partition)	$.15 \times 10^{-10}$
Grid Current (Shot)	$.02 \times 10^{-10}$
Flicker	$.43 \times 10^{-10}$
Battert	below 1.0×10^{-10}
Current	To be
Barkhausen	determined
Minimum Detectable Power	3.45×10^{-10}

* Values for a bandpass $\Delta f =$ 0.25cps.

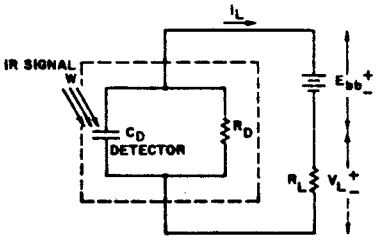

Fig. 1 Equivalent Circuit of a Ferroelectric Bolometer. C_D = Capacitance of the Detector, R_D = d.c. Ohmic Leakage of the Dielectric, R_L = Real Part of the Imput Impeadance of the Electrometer, E_{bb} = External Bias for the Detector, and W = Signal Imput to Detector.

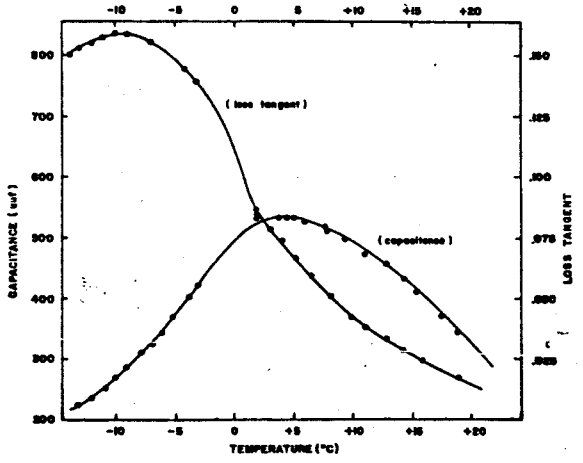

Fig. 2 Capacitance C_D and Loss Trangents as a Function of Temperature for the Ferroelectric Bolometer Serial No.G – 20311. Measurements at a Frequency of 1,000 cps. and a Field of 100 volt cm^{-1}

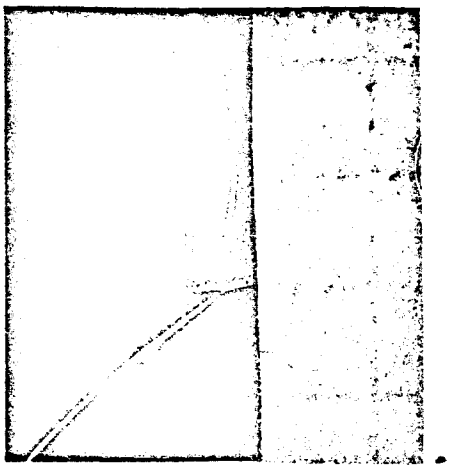

Fig. 3 Ferroelectric Bolometer Flake prior to Sealing. The Square Pattern , 1 mm x 1 mm is for Comparison Purpose

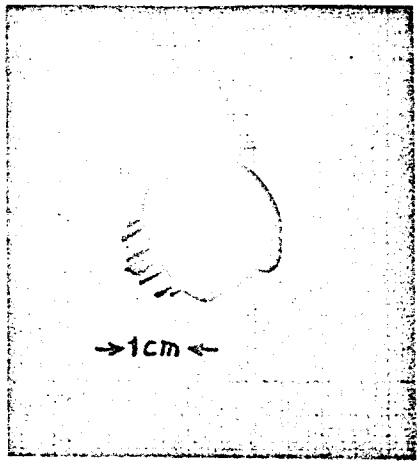

Fig. 4 Complete Ferroelectric Bolometer developed at Harvard College Observatory

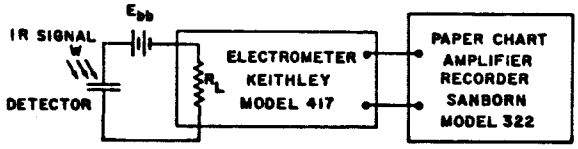

a) D.C. MODE OF OPERATION

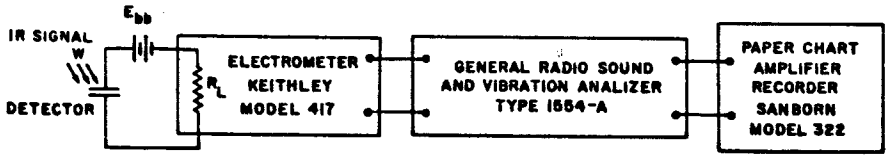

b) A.C. MODE OF OPERATION

Fig. 5 Block Diagrams at the Electronic setup for Testing the Ferroelectric Bolometer;

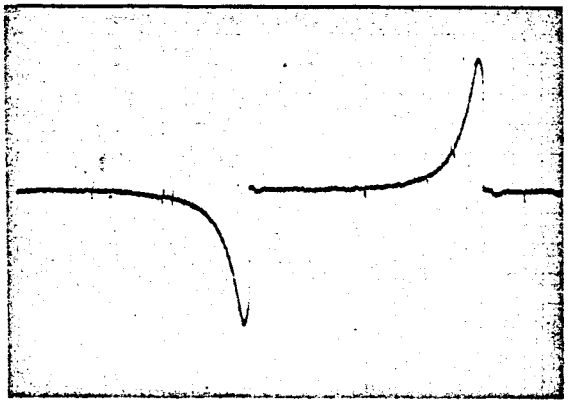

Fig. 6 Ferroelectric Bolometer, 1.0 mm x 1.0 mm in size, DC operation, 330 Volts Biasing, Room Temperature 28.5°C, Chart Speed 1 mms^{-1} , Signal $\Delta W = 7.5 \times 10^{-8}$ Watts, Noise Level determined by the Electronics

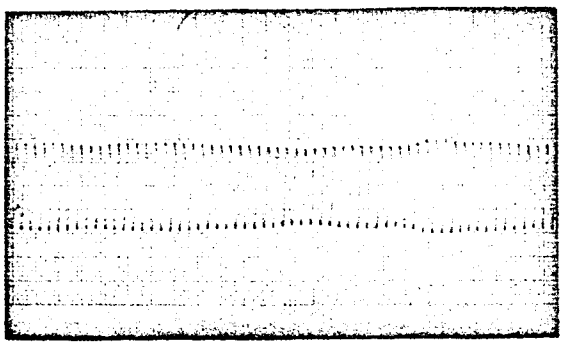

Fig. 7 The Same Conditions as in Fig. 6 but AC Operation, Signal $\Delta W = 5.8 \times 10^{-9}$ Watts Peak-to-Peak, Chopping Frequency 2.5 cps Bandwidth 0.25 cps.

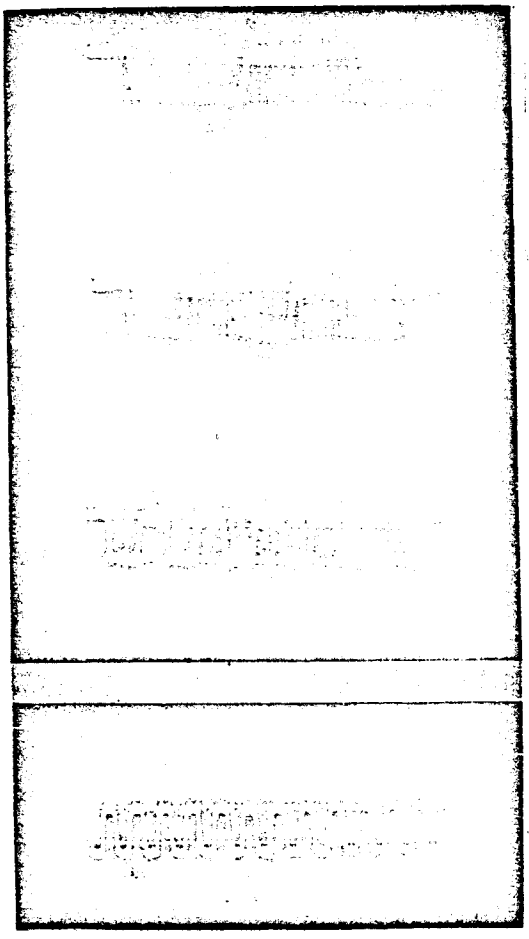

Fig. 8 The Same Bolometer as in Fig. 6, but at 120 Volts Biasing, Room Temperature 32°C and Chopping Frequencies of 0.78 cps, 1.56 cps, 3.3 cps and 6.2 cps respectively